Geothermics 39 (2010) 161–169

Contents lists available at ScienceDirect

Geothermics

journal homepage: www.elsevier.com/locate/geothermics

Electricity generation using a carbon-dioxide thermosiphon

Aleks D. Atrens*, Hal Gurgenci, Victor Rudolph

Queensland Geothermal Energy Centre of Excellence, The University of Queensland, Brisbane, QLD, 4067, Australia

ARTICLE INFO

Article history:
Received 10 June 2009
Accepted 1 March 2010
Available online 23 March 2010

Keywords:
Geothermal
Carbon dioxide
Thermosiphon
Enhanced geothermal systems
CO2
Exergy
Hot dry rock

ABSTRACT

There is an opportunity to expand the baseload geothermal electricity generation capacity through the development of engineered geothermal systems (EGS). Carbon dioxide (CO_2) could be used as an alternative to water to extract heat from these systems considering its advantages of ease of flow through the geothermal reservoir, strong innate buoyancy that permits the use of a thermosiphon rather than a pumped system over a large range of fluid flow rates, and lower dissolution of materials that lead to fouling. However, the thermodynamics of EGS using CO_2 to extract heat from subsurface rock masses is not well understood. Here we show that the wellbore frictional pressure losses are the dominant factor in CO_2-based EGS. Wellbore friction is the major limiter on the amount of energy that can be extracted from the reservoir by CO_2, as measured by the exergy available at the surface. The result is that CO_2 is less effective at energy extraction than water under conditions similar to past EGS trials. Nevertheless, CO_2 can perform well in lower permeability reservoirs, or if the wellbore diameter is increased. Our results demonstrate that CO_2-based EGS need to be designed with the use of CO_2 in mind. We suggest this work to be a starting point for analysis of the surface infrastructure and plant design and economics of CO_2-based EGS.

1. Introduction

The use of carbon dioxide (CO_2) as a heat extraction fluid in engineered geothermal systems (EGS) has been previously discussed (Brown, 2000; Pruess, 2006, 2008; Pruess and Azaroual, 2006; Gurgenci et al., 2008; Atrens et al., 2009a; Pritchett, 2009) as it offers a number of significant advantages as a geothermal heat extraction fluid, particularly:

- The non-polar fluid nature of CO_2, meaning salt solubility is low (decreasing the likelihood of scale precipitation in wellbores and surface equipment).
- Inherent physical sequestration of some CO_2 as part of the operation (amount needed to fill the reservoir volume), and depending on the geology present, possibility of chemically sequestering CO_2.
- Direct use of produced CO_2 fluid in turbomachinery is possible, making the process similar to that of a dry steam plant, instead of the binary designs typically proposed for EGS.
- A strong buoyancy effect, whereby the static pressure change in the injection well is much larger than in the production well, leading to self-driven high flow rates, making large pumping equipment unnecessary. A CO_2 thermosiphon, operating without a pump is illustrated in Fig. 1.
- Transport properties under reservoir temperature and pressure conditions, particularly viscosity and density, are favourable compared to water, promoting a higher rate of heat extraction.

Our previous work (Atrens et al., 2009a) modelled the performance and design of a hypothetical CO_2 thermosiphon, compared to a traditional water-based heat extraction system. The main findings were that under idealised conditions (no frictional pressure change in the wellbores, and a flow through a rectangular rock tube of constant height and width), CO_2- and water-based EGS would generate similar amounts of electricity, and that the one using CO_2 would be simpler in terms of surface equipment requirements.

That preliminary assessment contained a number of assumptions. Analysis of the CO_2 thermosiphon is extended here to include wellbore frictional pressure drop. We also update, clarify, and expand work discussed in a previous conference paper (Atrens et al., 2009b), by accounting for variation in width of the fluid flow path within the reservoir. We examine the exergy produced by CO_2 and water for a reference case, and the underlying characteristics of that performance. The effects of four individual significant changes from the reference case are also addressed: different impedance values, variation in the ratio of injection-to-production well numbers for a field-scale plant, shallower EGS, and wellbore diameter changes.

The goal of this assessment is to identify the subsurface parameters that have a significant influence on an EGS based on CO_2,

* Corresponding author. Tel.: +61 439 662 384; fax: +61 7 33654799.
E-mail address: aleks.atrens@uq.edu.au (A.D. Atrens).

0375-6505/$ – see front matter © 2010 Elsevier Ltd. All rights reserved.
doi:10.1016/j.geothermics.2010.03.001

Nomenclature

D	wellbore diameter (m)
f	friction factor
g	acceleration due to gravity ($m\,s^{-2}$)
H	height of reservoir (m)
h	enthalpy at wellhead ($kJ\,kg^{-1}$)
L	distance (m)
m	mass-flow rate ($kg\,s^{-1}$)
P	fluid pressure (Pa)
Re	Reynolds number
s	fluid entropy at wellhead ($kJ\,kg^{-1}\,K^{-1}$)
T_0	reference temperature (K)
V	fluid velocity ($m\,s^{-1}$)
W	width of fluid flow path in reservoir (m)
z	depth (m)

Greek symbols

Δ	change during a calculation step
ε	wellbore roughness (m)
κ	reservoir permeability (m^2)
μ	fluid viscosity (Pa s)
ρ	fluid density ($kg\,m^{-3}$)
Ψ	change in flow exergy between production and injection wellheads ($kJ\,s^{-1}$)

Subscripts

f	frictional
inj	injection
$prod$	production
res	reservoir
$well$	well

with the purpose of analysing the situations and designs that might effectively utilise this compound as the heat extraction fluid.

2. Methods

To understand the subsurface processes that influence CO_2- and water-based EGS, the injection and production components of the subsurface geothermal system are first examined separately. The injection component includes the injection well, or wells, and the fractured geothermal reservoir region through which the injected heat extraction fluid flows (hereafter referred to as the reservoir for brevity). The production component includes only the production well(s). The juncture between the two components of the EGS is at the base of the production well, where the pressure and temperature are equal to that of the reservoir.

The results discussed here were calculated using MATLAB. Because the computations for each component in the system are conducted at intervals of distance, the interval size was examined to determine its influence on accuracy. Increasing the number of intervals was found to have insignificant effect on the calculated results.

2.1. Injection

The temperature at the injection wellhead is assumed to be that of the ambient. The wellhead injection pressure is a variable in the calculations, and for CO_2 the cycle is designed so the turbine exhaust pressure is equal to injection pressure and therefore no further compression is required after the fluid is cooled. The temperature and pressure at the feed zone (where the reservoir fluid enters the production wells) were set equal to the reservoir temperature and pressure.

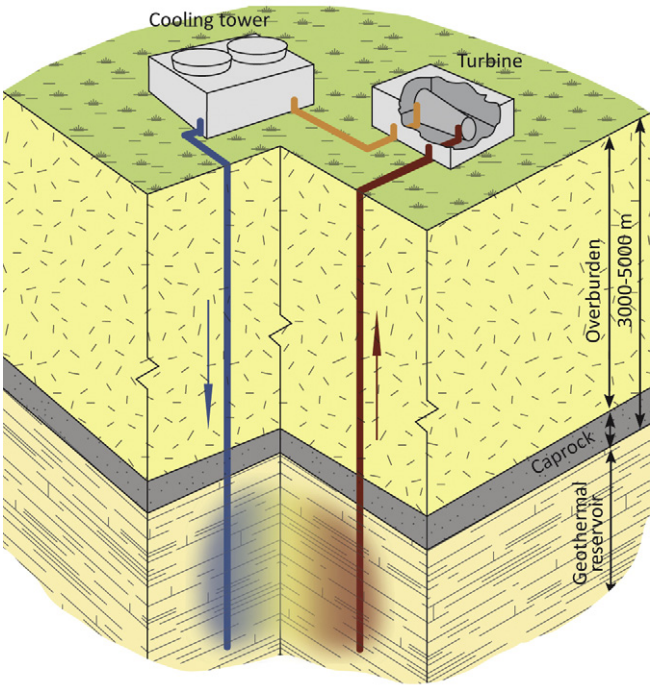

Fig. 1. An example of a CO_2 thermosiphon, a system designed to extract heat from geothermal reservoirs without pumping equipment.

The injection component of the studied system (Fig. 2) is characterised by the relationship between the injection pressure and the mass flow, which is derived from the fluid mechanics of pipe flow (White, 2008) in the injection well, and Darcy flow in the reservoir. This relationship is evaluated numerically using the equations of state for CO_2 and water based on Helmholtz free energy correlations (IAPWS, 1996, 2003, 2007; Span and Wagner, 1996; Vesovic et al., 1998). These high-accuracy correlations cover the thermodynamic and transport properties of these fluids over the range of temperatures and pressures considered in this work. The relationship is evaluated iteratively until the calculated reservoir pressure matches the defined reservoir pressure. The details of the numerical calculation are described below, with the results of the calculations presented in Fig. 3.

Calculations are based on the assumptions of steady-state operation, no work performed by the fluid, no heat flow across the boundaries of the wellbore, and constant well surface roughness for friction factor calculation. Pressure change is calculated based on standard pipe flow (White, 2008), and enthalpy change is derived from the first law of thermodynamics. Starting at the injection wellhead, an injection pressure P_{inj}, and a mass-flow rate, m are set. The change in fluid properties is then calculated at $\Delta z = 50$ m intervals along the injection borehole, from:

$$\Delta P = \rho g \Delta z - \Delta P_{f,well} \tag{1}$$

$$\Delta P_{f,well} = f \frac{\Delta z}{D} \rho \frac{V^2}{2} = f \frac{8 m^2 \Delta z}{\pi^2 \rho D^5} \tag{2}$$

$$f = \left\{ -1.8 \log \left[\frac{6.9}{Re} + \left(\frac{\varepsilon}{3.7D} \right)^{1.11} \right] \right\}^{-2} \tag{3}$$

$$\Delta h = g \Delta z - \frac{\Delta(V^2)}{2} \tag{4}$$

$\Delta P_{f,well}$ is the frictional pressure drop along the wellbore, P is the fluid pressure, ρ the fluid density, g the acceleration due to gravity, Δz the change in depth within the well, D the well diameter, ε the wellbore roughness, Re the Reynolds number, f the friction factor,

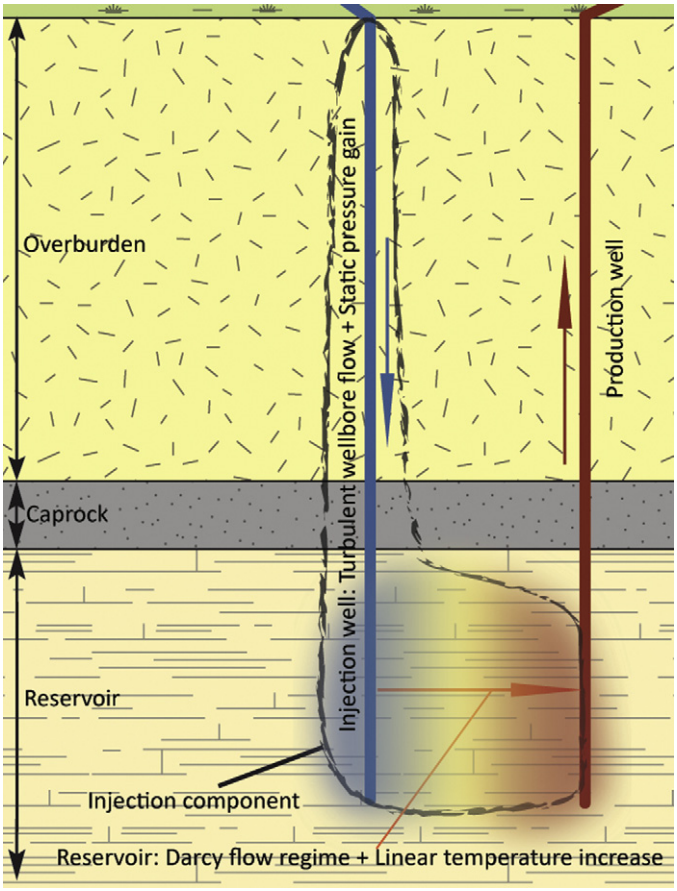

Fig. 2. Injection component of the system under study consisting of the injection well and the reservoir.

Δh the change in fluid enthalpy, and V the fluid velocity. Reynolds numbers are generally of the order of 10^6 in the injection well, and 10^7 in the production well, but depending on the process characteristics can range from 8×10^5 to 1×10^8, justifying the use of Eq. (3) to calculate the friction factor.

Fluid enters the reservoir at the base of the injection well. The pressure drop through the reservoir is calculated at 10 m intervals over the distance from the injection well to the production well, using the equation:

$$\frac{\Delta P_{f,res}}{\Delta L} = \frac{m\mu}{\rho\kappa HW} \quad (5)$$

where μ is the fluid viscosity, κ the reservoir permeability, H the reservoir height, W the width of the flow path in the reservoir, and ΔL the distance interval (i.e. 10 m). The calculated pressure at the exit of the reservoir is compared to the defined reservoir pressure. If they are different, either the injection pressure or mass-flow rate is changed, then the exit pressure recalculated. This is repeated until the square of the difference between the two reservoir pressures is less than 0.00005 (equivalent to a maximum percentage difference of 0.0025% in this study).

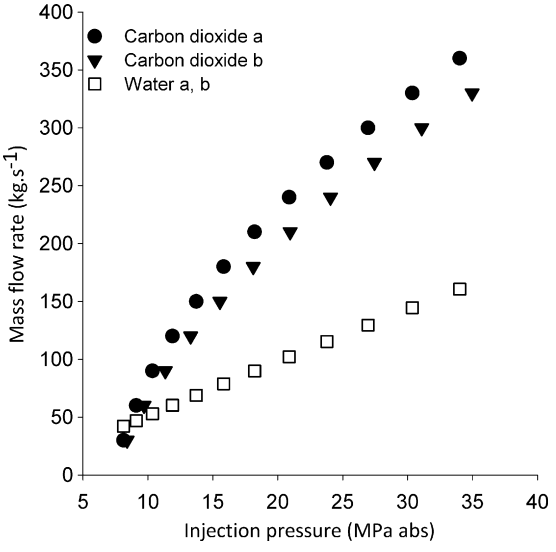

Fig. 3. Mass-flow rate into injection well versus injection wellhead pressure for a reservoir hydraulic impedance of 0.2 MPa s L^{-1}. (a) For varying reservoir flow-path width (see text); (b) for a constant flow-path width.

2.1.1. Reservoir shape

The reservoir parameters κ, H and W are not known. However, the hydraulic impedance for the reservoir (i.e. the pressure drop between the injection and production wells divided by the water flow rate) in past EGS trials has been between 0.2 and 1.0 MPa/(L s^{-1}) of water flow (Murphy et al., 1999). More recent EGS tests reflect this—e.g. a closed-loop circulation test in the Cooper Basin, Australia, had an impedance of 0.71 MPa/(kg s^{-1}) of water flow (Wyborn, 2009). After selecting a value for hydraulic impedance within this range, κ, H and W are calculated using an iterative procedure.

A lumped-parameter representation of the reservoir is used, with uniform values for κ and H throughout the volume. In spite of using constant κ and H, the width of the flow path, W is varied to represent the fluid flow through a hydrofractured zone. The effects of this variation were examined by comparing results using a uniform value for W, and a case where the width increases linearly with distance from the injection and production wells, to a maximum at the midpoint of the reservoir. The results of this comparison are given in Fig. 3, which shows the flow rate of water and CO_2 through the modelled EGS reservoir for a given wellhead injection pressure.

Obviously, the injectivity of water (i.e. the relationship between injection pressure and mass-flow rate) is unaffected by the choice of width, because the hydraulic impedance is kept constant. In contrast, the CO_2 injectivity changes when varying the width of reservoir flow path, due to the increased importance of the reservoir near-wellbore region. Most of the pressure drop occurs near the wellbore where the fluid velocity is greatest.

At low temperatures (i.e. near the injection wellbore) CO_2 has a much lower viscosity than water. This leads to a smaller pressure drop near the injection wellbore and consequently larger CO_2 flow rates than when water is used. The quantitative effect of modelling the reservoir with a varying flow path width instead of assuming one that is constant appears to be relatively small. This implies that if the reservoir is characterised by its hydraulic impedance, the geometry used for flow calculations has small effects on the injectivity of CO_2. Since the flow paths within actual reservoirs are likely to vary in width, non-uniform flow paths are used in the models discussed below.

2.1.2. Assumptions

The analysis described in this paper is based on steady-state conditions and on a number of assumptions:

- The reservoir has been assumed to be homogeneous, which is unlikely to be the case in reality. This was made due to the availability of flow data only, as overall mass-flow and overall pressure drop through the reservoir.
- The effects of localised changes in permeability on CO_2 and water flows have not been examined in this work, but may be viewed as

equivalent to localised changes in width, which has been found here to have some effect on the results.

- Hydraulic impedance measurements for water have been assumed to provide numerical values for reservoir characteristics that are suitable to apply to CO_2 flows. This is reasonable because the hydraulic impedance for water depends on the physical characteristics of the reservoir, and their relationship to the fluid properties of water flow as defined by the Darcy flow law (Eq. (5)). This assumption also reflects the lack of data for CO_2 flow through geothermal reservoirs.
- Heat transfer from the wells to the surrounding rock is neglected. For the injection well, this is reasonable due to the limited temperature difference between the borehole and the surrounding rock over most of the length of the well, and the generally poor conductivity of the rock. Heat transfer to the surroundings is expected to be higher in the production well than the injection well due to the larger temperature difference between the production well and the surrounding rock, but for the same reasons it is still expected to be low. Any heat losses in the production well will also be smaller for the CO_2 thermosiphon than for the water-based EGS, due to the lower temperatures of the CO_2 flow, leading to smaller driving forces for heat transfer.
- Finally, in the model the reservoir fluid temperature is assumed to follow a linear temperature increase with distance from the injection well in order to simplify the calculation. In reality, the temperature profile in the reservoir changes throughout the life of the EGS project. However, a general model of low temperatures near the injection well, and high temperatures near the production well is likely to be valid throughout the commercial operation period. As most of the reservoir pressure drop occurs in regions near the injection and production wells, changes in the temperature profile in other areas of the reservoir have only second-order effects.

2.2. Production well

Fluid transfer from the feed zone to the wellhead is modelled by pipe flow in the production well, in which the production pressure, P_{prod} is calculated from:

$$P_{prod} = P_{res} - \rho g \Delta z - \Delta P_{f,well} \quad (6)$$

where P_{res} is the reservoir pressure. The frictional pressure drop in the production well is calculated in the same manner as for the injection well, using Eqs. (2) and (3). The fluid enthalpy change is calculated from Eq. (4). The temperature and pressure of CO_2 and water in the production well are presented in Fig. 4.

Although Eqs. (2), (3) and (6) are the same for both water and CO_2, the two fluids undergo significantly different changes in temperature and pressure in the well between the feed zone and the wellhead due to their dissimilar thermodynamic properties. Under the conditions considered in this study, water has liquid-like properties, causing the decrease in enthalpy due to the change in gravitational potential energy to result almost solely in a decrease in production pressure. In contrast and as CO_2 has gas-like properties the decrease in enthalpy affects its temperature, volume, and pressure. Because some of the CO_2 enthalpy decrease is accounted for in a temperature decrease, the drop in production pressure is lower for CO_2 than for water.

Combining Eqs. (2), (3), (4) and (6) allows calculation of the production wellhead pressure for any mass-flow rate. Fig. 5 illustrates the influence on production pressure of increasing mass-flow rate. A higher flow lowers water production pressure, while for CO_2 there is a decrease in production pressure as well as a significantly lower temperature.

Carbon dioxide is produced at higher pressures at any mass-flow rate, and reaches larger overall flow rates than water. The high CO_2 production pressures are part of the buoyancy effect, and are higher than injection pressures. However, as production rates increase, the production pressure of CO_2 decreases rapidly. At the largest flow rates, due to increasing frictional pressure drop, the production pressure is reduced to the injection pressure required to sustain flow-rate, and further increases in flow cannot be achieved by the buoyancy effect (i.e. a pump or compressor is required). As discussed later in this work, those flow-rates are far above those desirable for effective exergy extraction.

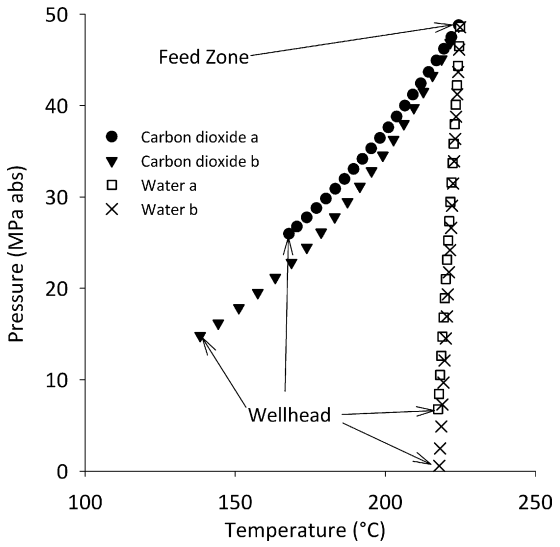

Fig. 4. Pressure-temperature conditions prevailing in the production wellbore. (a) 30 kg s^{-1}; (b) 200 kg s^{-1}.

3. Reference case

The injection and production analyses can be combined into one overall assessment, to calculate the exergy available for power generation in the geothermal power plant. The mass flow of the system and therefore the production pressure can be obtained based on a defined injection pressure, allowing the direct calculation of surface exergy change, Ψ, i.e.,

$$\Psi = m\left[h_{prod} - h_{inj} - T_0\left(s_{prod} - s_{inj}\right)\right] \quad (7)$$

where h_{prod} and s_{prod} are the enthalpy and entropy of the fluid exiting the production wellhead, h_{inj} and s_{inj} are the enthalpy and

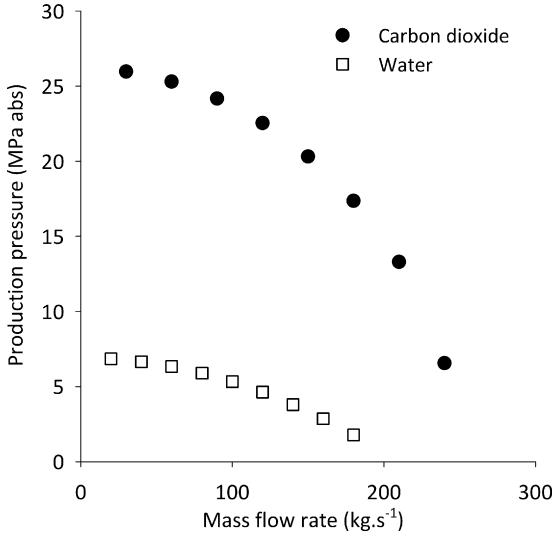

Fig. 5. Production wellhead pressure versus mass-flow rate.

Table 1
Reference parameters.

Depth	5000 m
Reservoir length	1000 m
Reservoir temperature	225 °C
Injection temperature	25 °C
Reference temperature	25 °C
Minimum reservoir flow-path width (well perimeter)	0.73 m
Maximum reservoir flow-path width	250.73 m
Impedance	0.2 MPa s L^{-1}
Corresponding $\kappa \cdot H$	8.603×10^{-11} m^3
Reservoir pressure	49.05 MPa
Wellbore roughness	4×10^{-4} m
Wellbore diameter	0.231 m

entropy entering the injection wellhead, and T_0 is the reference temperature (i.e. the ambient temperature).

The exergy flow indicates the maximum theoretical power that can be generated from the surface fluid flow under ideal conditions. In reality, the exergy flow will not directly match the amount of power that is generated, as it depends directly on the detailed design of the surface equipment. Because CO_2 and water will not have the same thermodynamic properties at the production wellhead, different systems are used to generate power. Carbon dioxide is likely to be sent directly into a turbine (because it is in a supercritical gas-like state), whereas a binary power cycle is expected for water (for EGS it is expected to be liquid-phase).

Even though the actual power generated depends on the efficiencies of the power plants being utilised, the exergy provides a convenient measure for the potential power generation as it gives some indication of power being produced without making assumptions about plant design. The parameters outlined in Table 1 were used for the analysis. Note that minimum reservoir flow-path width indicates the width available to flow in the reservoir at the edge of the wellbore, and is equal to the wellbore perimeter.

This set of reference parameters leads to the relationship of exergy produced versus injection pressure as presented in Fig. 6. Note that the exergy presented in this and following figures is normalised on a per well basis to account for the varying number (i.e. non-doublet) of wells in Section 5; i.e. to calculate the total exergy produced by each doublet, multiply the exergy by two.

As the injection pressure is increased, more fluid is injected into the system, and therefore more fluid is extracted from the production well. For water, raising the injection pressure leads to larger pumping requirements, but continually increases the heat recovered. For CO_2, higher injection pressures lead to larger production flows, which result in rapidly increasing drops in production wellhead pressures. The decreasing production pressures increases the production entropy, causing the produced exergy to reach a maximum, and then decrease with injection pressure, as seen in Fig. 6.

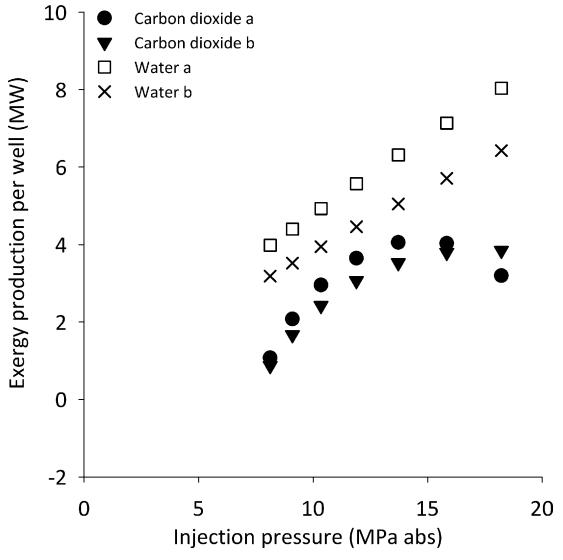

Fig. 6. Wellhead fluid exergy flows for CO_2 and water. (a) For reference case given in Table 1; (b) with 20% fluid loss.

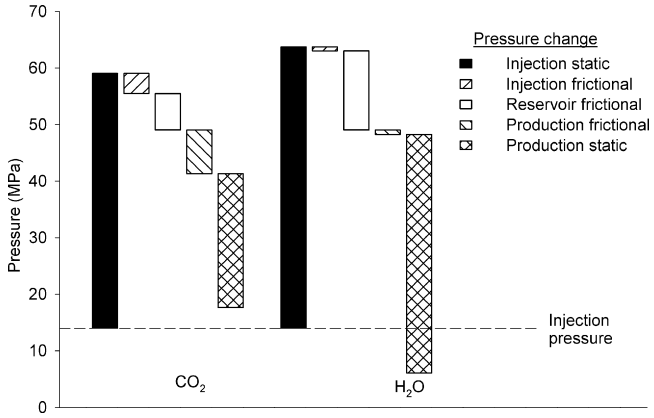

Fig. 7. Component pressure changes through the subsurface of the system for CO_2 and water for an injection pressure of 14 MPa.

The pressure changes for water and CO_2 through the subsurface sections of the EGS are shown in Fig. 7. The two fluids are each injected at 14 MPa, roughly corresponding to peak exergy production for CO_2; this leads to flow rates of 70.2, and 154.2 kg s^{-1} for water and CO_2, respectively.

From Fig. 7 it can be seen that the largest frictional pressure drop component for water is within the reservoir. For CO_2 the main frictional losses are in the production wellbore, which are significantly higher due to the larger flow rates and lower density. Also evident in this figure, even at a high CO_2 flow rate, is that the pressure decrease through the system is less than the static pressure gain in the injection well, with the remaining pressure difference allowing for direct power generation. In contrast, water is produced at a lower pressure than needed for re-injection, and will require pumping to sustain flow. This self-driven behaviour of CO_2 continues at higher fluid flow rates until the pressure losses are equal to the static pressure gain, although higher rates are undesirable due to lower exergy production.

Fluid losses from the reservoir to the surrounding rock (i.e. injected fluid that is not recovered in the production well) will not be examined comprehensively here, as they are site-dependent and the relationship between fluid properties and losses is unclear. However, by assuming that fluid losses have no effect on hydraulic reservoir impedance, a general view of their effects can be obtained. Fig. 6 (case "Water b") shows what happens when 20% of the fluid is lost at or near the production well feed zone (the value of m used in Eq. (6) is reduced by 20%). This change lowers the production fluid flow by 20%, which affects the frictional pressure drop in the production well, and the exergy available at the wellhead. Note that this approach assumes a steady-state system, implying that additional make-up fluid is supplied at the injection wellhead (at identical injection conditions). Therefore the reservoir pressure drop is unaffected, so the relationship between injection pressure and injected mass-flow rate remains the same. This simplified loss scenario provides some insight into the potential effects on the EGS project.

For the reference case, and variations in reference parameter values of ±20%, the system using CO_2 produces less exergy than the one based on water. The performance of the two systems may be comparable under a number of alternative cases:

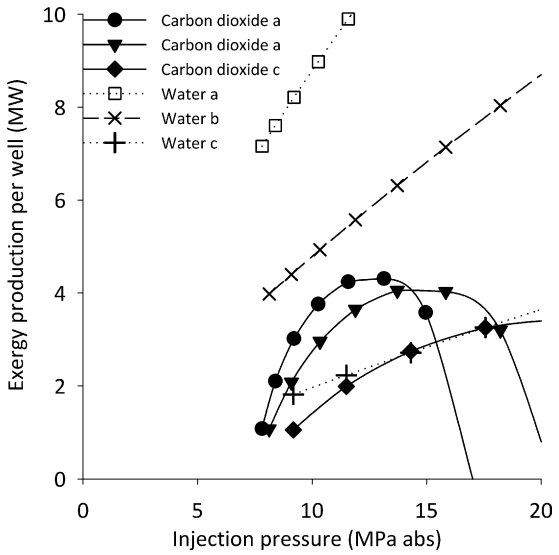

Fig. 8. Exergy produced versus injection pressure for different reservoir hydraulic impedance cases. (a) Impedance of 0.1 MPa s L^{-1}; (b) 0.2 MPa s L^{-1}; (c) 0.5 MPa s L^{-1}.

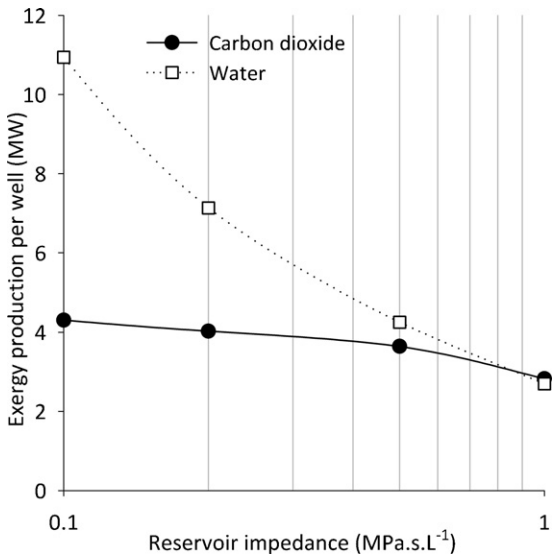

Fig. 9. Maximum exergy production of CO_2 for different reservoir properties, with corresponding exergy production of water at equal injection pressure (see text).

- High-impedance reservoirs.
- Field management where the ratio of the number of injection-to-production wells is different than 1:1.
- Shallow engineered geothermal systems.
- Large-diameter wellbores.
- These cases are addressed below.

4. High-impedance reservoirs

EGS systems based on CO_2 have the advantage of lower reservoir pressure drops than that those using water. For water-based EGS, reservoir pressure drop is the major component of impedance. Therefore it may be expected that in less permeable, higher impedance EGS reservoirs, CO_2 may perform more favourably compared to water than it does in the reference case. However, overall performance of both fluids would be expected to drop as impedance increases. The effect of variations in reservoir hydraulic impedance is shown in Fig. 8.

As hydraulic impedance increases, the performance of both fluids drops, although that of CO_2 decreases by a much smaller proportion compared to water. In a less permeable reservoir, the two fluids produce almost identical wellhead exergies over a range of typical operating conditions. In contrast, increasing reservoir permeability enhances the performance of the water-based EGS, but much less so for CO_2-based EGS. While utilising water and increasing injection pressure can partly offset a decrease in permeability, there are physical pumping limitations and high-pressure equipment is significantly more expensive.

A generalised comparison of the two fluids over a range of possible impedances is given in Fig. 9. This shows the maximum exergy produced by CO_2 versus reservoir impedance. A corresponding exergy production for water is also shown, which is calculated by using the injection pressure required to achieve maximum exergy production for the CO_2-based EGS. As the reservoir properties trend towards the limit of high impedance, the two fluids exhibit similar performance characteristics. However, as the reservoir is stimulated, there is decreased impedance and enhanced effective permeability, resulting in a vastly increased comparative performance in water flows.

The costs and benefits of stimulation procedures and duration will not be examined here. The different hydraulic impedances we discussed can be regarded as indicative of the reservoir before and after stimulation. The method and quantity of stimulation required to modify hydraulic impedance is a complex topic and might be the focus of future studies.

The use of CO_2 as a stimulation fluid is a subject that needs research. Past stimulation of EGS has used water. Readers interested in stimulation of EGS reservoirs are referred to Evans et al. (2005), Baisch et al. (2006), and Zimmermann et al. (2010).

5. Injection-to-production well ratio

Most exergy losses in the CO_2 thermosiphon occur in the production wellbore. These losses increase rapidly with increasing flow rate. By contrast, pressure drop and exergy losses in the injection well are lower, and not as negatively impacted by flow-rate increases. Therefore performance can be expected to improve by operating a plant with more production wells than injection wells, effectively reducing the flow rates in individual production wells while increasing those in the injectors.

This approach will be cost-neutral if the total number of wells is kept constant, and only the number of injection- to-production well ratio is changed. Note that this analysis is for the case of a field development consisting of many wells, not for a doublet or other small grouping. The consideration here is not of the value of drilling additional wells, but whether in an overall field of many wells, it is preferable to have more injection than production wells. Exergy production is divided by the total number of wells to normalise the result (and remove the need to consider factors such as well cost). The total exergy produced by the CO_2 thermosiphon divided by the total number of wells is shown in Fig. 10 for different ratios of injection-to-production wells.

Decreasing the ratio of injection-to-production wells marginally enhances the performance of the CO_2 thermosiphon, although this improvement is offset by a higher wellhead injection pressure. This change is not relevant when handling a small number (up to five) wells, but becomes important when managing more wells in a large-scale geothermal field development is considered. The results shown in Fig. 10 suggest that there will be some advantage in additional analysis of this reduction in well ratio for specific sites. Ratios below 1:1 may also cause the heat extraction fluid to flow through a larger area of the reservoir (e.g. applicable for the development scenario where a small number of central injection wells are ringed by a larger number of producers). This may reduce the reservoir (and

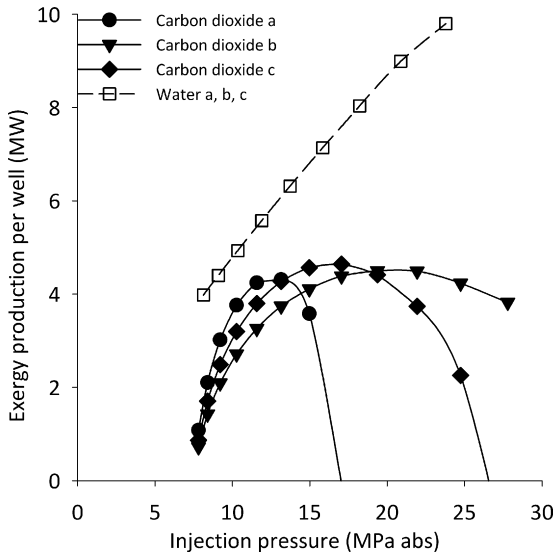

Fig. 10. Effect on exergy production when changing the injection-to-production wells ratio. Injection/production ratios: (a) 1:1; (b) 1:2; (c) 2:3.

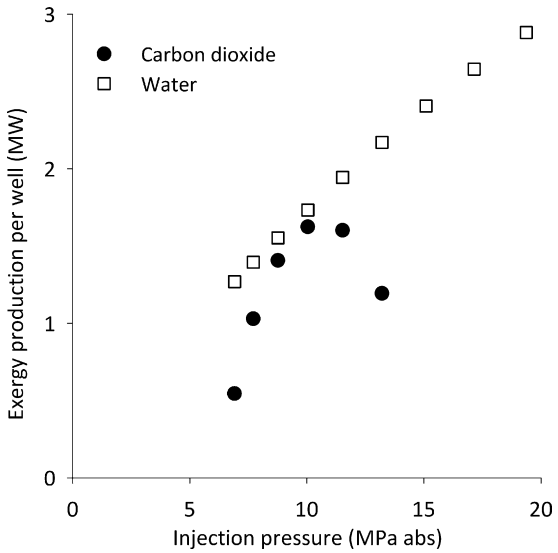

Fig. 11. Performance of a shallower Engineered Geothermal System (EGS).

fluid production) temperature decline over time, and decrease fluid losses, but an accurate prediction requires more in-depth analysis of fluid flow in the reservoir.

6. Shallow engineered geothermal systems

There are EGS opportunities that are shallower than the reference case (Section 3); they are typically also of lower temperature. These systems are less likely to be suitable for using CO_2 as the heat extraction fluid due to the higher likelihood of connectivity to the water table at shallow depths; only if adequate cap rocks are present CO_2 should be considered. Even though these shallow systems may produce less electricity because of the lower temperature resources involved, they may be competitive due to reduced well drilling costs.

The smaller well depth leading to reduced importance of wellbore pressure losses would preferentially improve the performance of CO_2 thermosiphon over water-based systems. The high dependence of water viscosity on temperature would also favour the use of CO_2 in low-temperature systems. The performance of CO_2- and water-based EGS for a resource of 150 °C at 3000 m depth is shown in Fig. 11. All other parameters are identical to the reference case.

In a shallower EGS the CO_2 thermosiphon produces marginally less exergy than the water-based system. As expected, exergy production is lower than for the reference case, although the magnitude of this difference will vary on a case-by-case basis. The marginal difference is unlikely to severely disadvantage the utilisation of CO_2, which can leverage off the reduced surface equipment required for the system. A CO_2-based EGS may operate competitively with a simple design and low injection pressures in a shallow, low-temperature EGS.

7. Large-diameter wellbores

Changing the wellbore characteristics (diameter and roughness) has the potential to reduce frictional losses for the CO_2 thermosiphon and improve its performance. These changes will have minor effects on water-based EGS due to the already small wellbore frictional pressure drops. Changes to these characteristics, particularly diameter, will have a substantial effect on capital cost.

A reduction in wellbore surface roughness in the wellbore will lower frictional pressure losses for CO_2-based systems. The effect, however, is small, with a less than linear relation to pressure drop, so is not discussed in detail here. Utilising low roughness casing may be worthwhile for a CO_2 thermosiphon, but the reality of retaining low roughness pipe exposed to turbulent (and potentially erosive or corrosive) fluid flow is open to speculation.

A larger impact on the flow regime can be accomplished through larger diameter wellbores, which may cost more, but will have a significant effect on the operation of the CO_2 thermosiphon. Fig. 12 shows the impact on exergy production when the wellbore diameter is increased. Note that this effect has been examined for both the CO_2 thermosiphon and for the water-based EGS, but for water there is no evident difference. Similarly, the improvement of CO_2 performance with increased diameter will diminish at larger values, but the limit will be defined by practical/technological limitations and by well drilling and completion costs.

Fig. 12 shows that CO_2 will produce similar quantities of exergy to a water-based EGS if larger wellbores are used. Depending on the increase in diameter, exergy production of the CO_2 thermosiphon

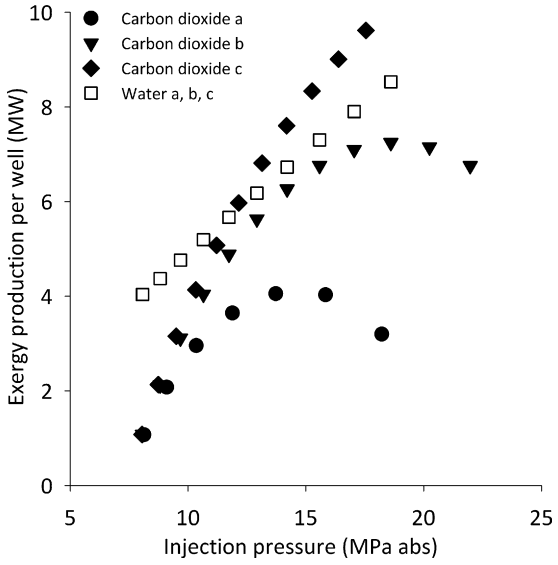

Fig. 12. Effect of increasing wellbore diameter on exergy production; (a) 23.5 cm (9.25 in.) diameter; (b) 30.5 cm (12 in.) diameter; (c) 40.6 cm (16 in.) diameter.

may surpass that of the water-based EGS over the reasonable range of wellhead conditions.

8. Discussion

A number of assumptions have been discussed in relation to their effect on some components of an Engineered Geothermal System (i.e. no heat transfer in the wellbores, and a linear temperature profile in the reservoir). In addition, the overall study is based on a number of more general assumptions that have broader impacts on the injection-production scenarios modelled. These assumptions are: a constant (i.e. uniform) reservoir permeability, no fluid losses (except in the one case examined), and the pressure at the feed zone being equal to the reservoir pressure. It is worth reviewing each of these in detail. The effect on the modelled scenario of varying the parameters for impedance, injection-to-production well ratio, wellbore diameter, and reservoir depth are discussed in Sections 4–7.

Fluid flows in the reservoir have been modelled for a case where the permeability has a constant value throughout the reservoir, and depends on the physical properties of the rock, determined from overall hydraulic impedance. This is in contrast to some past EGS trials (Murphy et al., 1999), where the calculated impedance was decreased as injection pressure was increased. The cases examined here are at much higher flow rates (i.e. order of magnitude greater) and injection pressures than in the past EGS tests where there was a dependence of impedance on injection pressure. It is considered that impedance is likely to reach a limiting value that depends on the reservoir geometry (that is, fracture size, frequency, and tortuosity), at which point increasing pressure will have no noticeable effect on injection impedance or permeability. This work deals with high injection pressure and flows, such that the pressure-induced stresses on the rock are large enough to make impedance independent of pressure.

In this study, fluid losses into the rock mass surrounding the wellbores have been assumed to be negligible. This is in contrast to EGS tests (Brown et al., 1999), which in some cases had high losses of injected water (in one instance they amounted to 78%). In those cases, losses increased with injection pressures.

Although the discussed cases examine only doublets, it is assumed that for a commercial-scale EGS, the wells will be part of a larger field development. A large field with wells at regular intervals is likely to encounter lower fluid losses than an isolated pair of wells. To some extent, the consideration of losses is moot—if losses are a problem, the water-based EGS will operate with lower injection pressures and a downhole pump in the production well to minimise losses, whereas the CO_2 thermosiphon can accept losses as a beneficial sequestration effect. The concern over losses in some reservoirs will provide an upper limit on injection pressure for water, and may for CO_2 depending on availability of the fluid. Fluid losses are a topic of further interest to EGS in general, however, and better understanding of the likely amount of fluid loss, and the change in losses over time (particularly over several years or decades) is necessary before commercial implementation of any EGS in regions where injectate losses are likely.

The assumption that the pressure at the juncture of the reservoir and production well is equal to the reservoir pressure is linked with the above discussion. A CO_2 thermosiphon must be modelled with this constraint; if the pressure at the base of the production well is lower than that of the surrounding formation, there is a risk of fluids (i.e. water) entering from areas of the reservoir not filled with CO_2, or from rock layers above or below the targeted reservoir production zone. For water-based EGS, this assumption could be relaxed, but fundamentally does not affect the qualitative thermodynamic results. The assumption may influence the decision to incorporate in the design a down-hole pump inside the production well, or a surface pump at the injection wellhead, but this will affect the engineering and economics of the EGS project, but not thermodynamics. Overall this assumption on the pressure is necessary to appropriately analyse the CO_2 thermosiphon, and is reasonable for a water-based EGS. It is used for both fluids to minimise differences in the modelling studies.

9. Conclusions

The CO_2 thermosiphon produces less exergy than the water-based system for the reference case. This is despite the favourable CO_2 characteristics of low viscosity and innate buoyancy drive. The reason for this comparative underperformance is due to two key differences between CO_2 and water:

- Lower heat capacity of CO_2 than that of water, leading to much larger CO_2 flows required for a similar rate of heat extraction from the subsurface rock.
- The much lower density of CO_2 in the production wellbore due to its supercritical/gaseous nature at the temperature and pressure prevailing in the wellbore.

Both characteristics lead to significantly larger pressure drops in the production well for CO_2 compared to water, which is coupled with an associated temperature decrease due to Joule–Thompson expansion. Both the decrease in pressure and temperature reduce the exergy available at the wellhead to generate electricity.

From the range of different process conditions and reservoir parameters considered, the following observations can be made:

- The two disadvantages just mentioned above are dominant for the different cases examined, leading to CO_2 extracting less exergy than water.
- CO_2 displays a similar exergy production to water in high-impedance reservoirs and in shallow EGS.
- The performance of CO_2 is considerably increased by using large-diameter wellbores, to the point where the difference in production compared to water is insignificant. This depends on other characteristics of the system, but is broadly true for the range of cases examined here, and are expected to apply to EGS using CO_2 in general.

This analysis provides a broad overview of the significant differences present in an EGS that utilises CO_2 instead of water. While some simplifying assumptions are included, they are expected to be of a second-order nature compared to the dominant effects discussed here. As such, this work provides a foundation for the design and analysis of geothermal power plants associated with CO_2-based Engineered Geothermal Systems.

The selection of any process design depends on an economic assessment; this is true also of the CO_2 thermosiphon. Economics have not been considered here, but some conclusions can be drawn as to the likely parameters impacting CO_2-based EGS economic viability, and the reservoir characteristics under which CO_2 performs most competitively. It can be seen that:

- The dominant consideration for the usage of CO_2 in geothermal systems is wellbore pressure drop. EGS aimed at using CO_2 need to account for this in their design.
- CO_2 may be suitable and competitive for shallower EGS or low-permeability EGS due to power generation similar to water and simpler process design.
- The advantages of CO_2 over water as a reservoir heat exchange fluid are not pronounced unless it becomes feasible to drill larger

wells. However, even with the present well sizes, CO_2 thermosiphon may be preferred because there are no heat exchanger losses at the surface since the CO_2 is sent directly from the wellhead to be run through the turbine. In this context, the power generating system associated with a CO_2 thermosiphon would be similar to a dry-steam geothermal plant, with all the advantages of such installations.

Acknowledgments

We acknowledge the support of the Queensland State Government whose funding of the Queensland Geothermal Energy Centre of Excellence made this work possible. We also thank Andrejs Atrens for useful discussion and comments.

References

Atrens, A.D., Gurgenci, H., Rudolph, V., 2009a. CO_2 thermosiphon for competitive power generation. Energy & Fuels 23, 553–557.

Atrens, A.D., Gurgenci, H., Rudolph, V., 2009b. Exergy analysis of a CO_2 thermosiphon. In: Proceedings of the Thirty-Fourth Workshop on Geothermal Reservoir Engineering, Stanford University, Stanford, CA, USA, 6 pp.

Baisch, S., Weidler, R., Voros, R., Wyborn, D., de Graaf, L., 2006. Induced seismicity during the stimulation of a geothermal HFR reservoir in the Cooper Basin, Australia. Bulletin of the Seismological Society of America 96, 2242–2256.

Brown, D., Robert, D., Kruger, P., Swenson, D., Yamaguchi, T., 1999. Fluid circulation and heat extraction from engineered geothermal reservoirs. Geothermics 28, 553–572.

Brown, D.W., 2000. A hot dry rock geothermal energy concept utilizing supercritical CO_2 instead of water. In: Proceedings of the Twenty-Fifth Workshop on Geothermal Reservoir Engineering, Stanford University, Stanford, CA, USA, 6 pp.

Evans, K.F., Moriya, H., Niitsuma, H., Jones, R.H., Phillips, W.S., Genter, A., Sausse, J., Jung, R., Baria, R., 2005. Microseismicity and permeability enhancement of hydrogeologic structures during massive fluid injections into granite at 3 km depth at the Soultz HDR site. Geophysical Journal International 160, 388–412.

Gurgenci, H., Rudolph, V., Saha, T., Lu, M., 2008. Challenges for geothermal energy utilisation. In: Thirty-Third Workshop on Geothermal Reservoir Engineering. Stanford University, Stanford, CA, USA, 7 pp.

IAPWS, 1996. Release on the IAPWS Formulation 1995 for the Thermodynamic Properties of Ordinary Water Substance for General and Scientific Use. The International Association for the Properties of Water and Steam, Fredericia, Denmark, http://www.icpws15.de/IAPWS_documents/Releases/IAPWS95.pdf.

IAPWS, 2003. Revised Release on the IAPS Formulation 1985 for the Viscosity of Ordinary Water Substance. The International Association for the Properties of Water and Steam, Vejle, Denmark, http://www.icpws15.de/IAPWS_documents/Releases/visc.pdf.

IAPWS, 2007. Revised Release on the IAPWS Industrial Formulation 1997 for the Thermodynamic Properties of Water and Steam. The International Association for the Properties of Water and Steam, Lucerne, Switzerland, http://www.icpws15.de/IAPWS_documents/Releases/IF97-Rev.pdf.

Murphy, H., Brown, Jung, R., Matsunaga, I., Parker, R., 1999. Hydraulics and well testing of engineered geothermal reservoirs. Geothermics 28, 491–506.

Pritchett, J.W., 2009. On the relative effectiveness of H_2O and CO_2 as reservoir working fluids for EGS heat mining. Geothermal Resources Council Transactions 33, 235–239.

Pruess, K., 2006. Enhanced geothermal systems (EGS) using CO_2 as working fluid—a novel approach for generating renewable energy with simultaneous sequestration of carbon. Geothermics 35, 351–367.

Pruess, K., 2008. On production behaviour of enhanced geothermal systems with CO_2 as working fluid. Energy Conversion and Management 49, 1446–1454.

Pruess, K., Azaroual, M., 2006. On the feasibility of using supercritical CO_2 as heat transmission fluid in an engineered hot dry rock geothermal system. In: Proceedings of the Thirty-First workshop on Geothermal Reservoir Engineering, Stanford, CA, USA. Stanford University, 8 pp.

Span, R., Wagner, W., 1996. A new equation of state for carbon dioxide covering the fluid region from the triple-point temperature to 1100 K at pressures up to 800 MPa. Journal of Physical and Chemical Reference Data 25, 1509–1596.

Vesovic, V., Fenghour, A., Wakeham, W.A., 1998. The viscosity of carbon dioxide. Journal of Physical and Chemical Reference Data 27, 31–44.

White, F.M., 2008. Fluid Mechanics. McGraw-Hill, Boston, MA, USA, 864 pp.

Wyborn, D., 2009. Completion of Habanero closed-loop circulation test. In: Paper presented at the 2009 Australian Geothermal Energy Conference, 10–13 November, Brisbane, QLD, Australia.

Zimmermann, G., Moeck, I., Blöcher, G., 2010. Cyclic waterfrac stimulation to develop an enhanced geothermal system (EGS)—conceptual design and experimental results. Geothermics 39, 59–69.